physica status solidi rrl
www.pss-rapid.com

Check for updates

Atomic-Layer-Deposited Al_2O_3 as Effective Barrier against the Diffusion of Hydrogen from SiN_x:H Layers into Crystalline Silicon during Rapid Thermal Annealing

Lailah Helmich, Dominic C. Walter, Dennis Bredemeier, and Jan Schmidt*

Stacks of hydrogen-lean aluminum oxide, deposited via plasma-assisted atomic-layer-deposition, and hydrogen-rich plasma-enhanced chemical vapor-deposited silicon nitride (SiN_x) are applied to boron-doped float-zone silicon wafers. A rapid thermal annealing (RTA) step is performed in an infrared conveyor-belt furnace at different set-peak temperatures. The hydrogen content diffused into the crystalline silicon during the RTA step is quantified by measurements of the silicon resistivity increase due to hydrogen passivation of boron dopant atoms. These experiments indicate that there exists a temperature-dependent maximum in the introduced hydrogen content. The exact position of this maximum depends on the composition of the SiN_x layer. The highest total hydrogen content, exceeding 10^{15} cm^{-3}, is introduced into the silicon bulk from silicon-rich SiN_x layers with a refractive index of 2.3 (at $\lambda = 633$ nm) at an RTA peak temperature of 800 °C, omitting the Al_2O_3 interlayer. Adding an Al_2O_3 interlayer with a thickness of 20 nm reduces the hydrogen content by a factor of four, demonstrating that Al_2O_3 acts as a highly effective hydrogen diffusion barrier. Measuring the hydrogen content in the silicon bulk as a function of Al_2O_3 thickness at different RTA peak temperatures provides the hydrogen diffusion length in Al_2O_3 as a function of measured temperature.

Atomic-layer-deposited (ALD) Al_2O_3 films with a thickness of a few nanometers have been successfully applied in microelectronics and photovoltaics.[1–5] In particular, in silicon-based solar cells, the introduction of Al_2O_3 surface passivation layers was a crucial step towards higher efficiencies of industrial solar cells in recent years. The metal contacts in today's industrial silicon solar cells are made by screen-printing of metal pastes in combination with a subsequent rapid thermal annealing (RTA) step at set-peak temperatures in the range between 750 and 850 °C for a few seconds.[6] To preserve the excellent passivation quality of the ALD-Al_2O_3 layers on the silicon surface during the RTA step, the Al_2O_3 layers are capped by silicon nitride (SiN_x) layers. These top layers are grown by means of plasma-enhanced chemical vapor deposition (PECVD), resulting in amorphous SiN_x:H layer with very high hydrogen content (typically in the range of 10–20 at%).[7] In contrast, ALD-Al_2O_3 layers have a hydrogen content in the range of only 1–2 at%.[3] During the RTA step, hydrogen partly diffuses from the hydrogen-rich SiN_x layer[8] through the Al_2O_3 layer to the interface and also into the crystalline silicon bulk, where it is able to passivate defects.[9–11] Interestingly, the hydrogen was also found to be able to create new recombination centers in the silicon bulk, in some cases leading to a severe degradation in solar cell efficiency during illumination.[12–16] Therefore, in photovoltaics, the control of the amount of hydrogen diffusing into the crystalline silicon bulk has turned out to be of utmost importance. There have been conjectures in the literature that Al_2O_3 layers might severely hamper the in-diffusion of hydrogen from SiN_x:H into the silicon bulk.[17,18] However, these studies did not provide any quantitative measurements on how effective Al_2O_3 actually is as a hydrogen barrier. This letter aims at closing this gap by quantifying the amount of hydrogen diffused into the silicon bulk through Al_2O_3 layers of different thicknesses (5−25 nm) at varying RTA peak temperatures ϑ_{peak}.

Figure 1 shows exemplary measurements for three group A samples (see Experimental Section) with SiN_x:H films of different compositions, fired at a measured RTA peak temperature of (792 ± 10)°C. Directly after RTA, the hydrogen is mainly present in the form of hydrogen dimers H_2 in the silicon bulk.[19] These H_2 dimers dissociate during low-temperature annealing in darkness (e.g., at 160 °C) and the hydrogen atoms subsequently passivate boron dopant atoms.[20] As a consequence, the bulk resistivity ρ of the sample increases as a function of time during dark annealing at 160 °C on a hotplate. We measure the resistivities in-between the periods of 160 °C-dark annealing using

L. Helmich, Dr. D. C. Walter, Dr. D. Bredemeier, Prof. J. Schmidt
Institute for Solar Energy Research Hamelin (ISFH)
Am Ohrberg 1, Emmerthal 31860, Germany
E-mail: l.helmich@isfh.de

L. Helmich, Dr. D. Bredemeier, Prof. J. Schmidt
Department of Solar Energy
Institute of Solid-State Physics
Leibniz University Hannover
Appelstraße 2, Hannover 30167, Germany

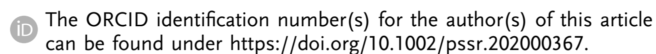
The ORCID identification number(s) for the author(s) of this article can be found under https://doi.org/10.1002/pssr.202000367.

© 2020 The Authors. Published by Wiley-VCH GmbH. This is an open access article under the terms of the Creative Commons Attribution-NonCommercial-NoDerivs License, which permits use and distribution in any medium, provided the original work is properly cited, the use is non-commercial and no modifications or adaptations are made.

DOI: 10.1002/pssr.202000367

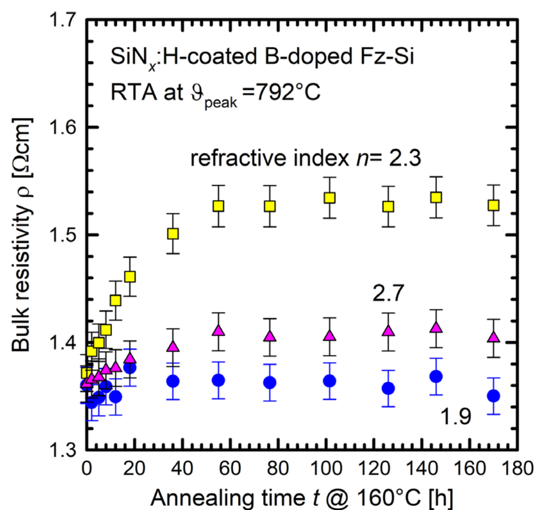

Figure 1. Measured evolution of the bulk resistivity ρ versus the annealing time at 160 °C in the dark of SiN_x:H-coated 1.4 Ω cm boron-doped float-zone silicon (Fz-Si) samples, rapid thermal annealing (RTA) treated at a measured peak temperature ϑ_{peak} of (792 ± 10)°C. The refractive index n of the SiN_x layer is varied between 1.9 (nearly stoichiometric SiN_x) and 2.7 (very silicon-rich SiN_x). Silicon-rich SiN_x layers with $n = 2.3$ result in the highest resistivity increase and hence the highest hydrogen concentration in the silicon bulk.

the eddy-current method by inductive coupling the sample to a WCT-120 bridge (Sinton Instruments). The sample temperature is recorded during each measurement and the resistivities are extrapolated to 25 °C, as described in detail by Walter et al.[21] The higher the saturation value of the measured base resistivity, the higher is the boron–hydrogen (BH) pair concentration and thus the hydrogen concentration in the silicon bulk. In a recent contribution,[21] it was shown that for silicon material of the used boron concentration, the saturated BH concentration can be identified with the total hydrogen content $[H_{tot}]$ in the silicon bulk. According to the study by Walter et al.,[21] the deviation from the true hydrogen content is less than 5% for the boron doping concentration applied in this article.

Figure 2a shows the measured total hydrogen concentration in the silicon bulk for three SiN_x layers with different compositions (corresponding to refractive indices of $n = 1.9$, 2.3, and 2.7) as a function of the measured peak temperature ϑ_{peak} of the RTA step. Whereas the nearly stoichiometric SiN_x layer with a refractive index of $n = 1.9$ results in the lowest hydrogen concentration $[H_{tot}]$ within the silicon bulk, increasing the silicon content in the SiN_x layer and thereby its refractive index of $n = 2.3$ significantly increases $[H_{tot}]$. A further increase in the silicon content of the SiN_x layers to $n = 2.7$, however, decreases $[H_{tot}]$ again. The maximum amount of hydrogen is hence introduced into the silicon bulk for the silicon-rich SiN_x layers with a refractive index of $n = 2.3$, in agreement with the recent findings of another study.[22] In addition, Figure 2a demonstrates that $[H_{tot}]$ critically depends on the peak temperature: At low peak temperatures, $[H_{tot}]$ increases with increasing ϑ_{peak}, whereas at high peak temperatures, $[H_{tot}]$ decreases with increasing ϑ_{peak}. The maximum of $[H_{tot}]$ as a function of ϑ_{peak} depends on the silicon content of

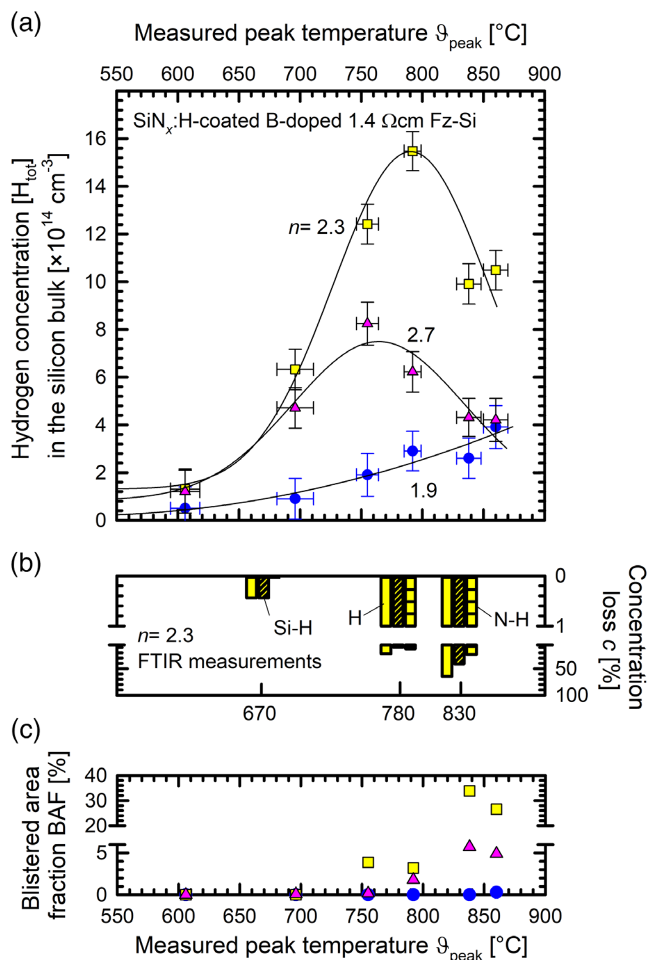

Figure 2. a) Total hydrogen concentration $[H_{tot}]$ of SiN_x-coated 1.4 Ω cm boron-doped float-zone silicon (Fz-Si) wafers after rapid thermal annealing (RTA) treatment as a function of the peak temperature ϑ_{peak} measured during rapid thermal annealing (RTA). The solid lines are guides to the eyes. b) Percentage loss of Si—H (middle bar) and N—H bonds (right bar) in the SiN_x:H layers ($n = 2.3$) obtained from Fourier-Transform Infrared Spectroscopy (FTIR) measurements, and the total hydrogen (left bar) loss (sum of Si—H and N—H losses, solid) versus ϑ_{peak}. c) Blistered area fraction (BAF) of the different SiN_x:H layers obtained from light microscopy images versus ϑ_{peak}.

the SiN_x layer. With increasing silicon content of the SiN_x layers, the maximum hydrogen content in the silicon bulk is detected at decreasing ϑ_{peak} values. Note that for the nearly stoichiometric SiN_x layers ($n = 1.9$), the maximum seems to lie outside of our experimental peak temperature window. The maximum total hydrogen concentration $[H_{tot}]$ of 1.5×10^{15} cm^{-3} is obtained at a peak temperature of (792 ± 10)°C for a silicon-rich SiN_x layer with $n = 2.3$. To understand the temperature dependences shown in Figure 2a, we have performed Fourier-Transform Infrared Spectroscopy (FTIR) measurements of the different bondings in the SiN_x:H layers with $n = 2.3$ before and after RTA. We use a BrukerVERTEX 70 FTIR spectrometer to measure the Si—N peaks at wavenumbers ν of 880 and 1030 cm^{-1}, the Si—H peak at $\nu = 2180$ cm^{-1}, and the N—H peak at $\nu = 3320$ cm^{-1}.[23] The evaluation of the peaks is performed by

© 2020 The Authors. Published by Wiley-VCH GmbH

using calibration constants from the study by Bredemeier et al.[23] Figure 2b shows the relative losses of Si—H and N—H bond concentrations and the total hydrogen content within the SiN_x:H layers as a function of the RTA peak temperature.

After the RTA step at a measured peak temperature of (670 ± 10)°C, only a negligibly small loss in the Si—H bond concentration (−0.4%) is observed, whereas the N—H bond concentration remains unchanged. Therefore, we can identify the total hydrogen loss in the SiN_x:H layer with the loss in the Si—H bonds. After the RTA step at $\vartheta_{peak} = (780 \pm 10)$°C, which is very close to the maximum hydrogen in-diffusion into the silicon bulk (see yellow squares in Figure 2a), the N—H bond concentration in the SiN_x:H film shows a pronounced decrease (−12.5%) as does the Si—H bond concentration (−9.4%). The overall hydrogen loss in the SiN_x:H layer amounts therefore to −21.9%, which is two orders of magnitude larger than the hydrogen loss measured at 670 °C. An RTA step at 830 °C peak temperature results in the highest overall hydrogen concentration loss of −64.3%. Both, the Si—H and the N—H bond concentrations show a pronounced decrease by −41.0% and −23.3%, respectively. Despite these huge hydrogen losses in the SiN_x:H layers during the RTA step, it should be kept in mind that the vast majority of hydrogen effuses into the atmosphere[24,25] and only a very small portion diffuses into the silicon bulk. Nevertheless, our FTIR measurements demonstrate that at low temperatures (<700 °C), the dissociation of the weaker Si—H bonds governs the overall hydrogen out-diffusion and therefore also the diffusion into the silicon bulk. The relative loss of hydrogen in the SiN_x:H layers is, however, very low (<1%) at the low peak temperatures, which in turn also results in low hydrogen concentrations introduced into the silicon bulk. At higher peak temperatures (>750 °C), Si—H and N—H bonds dissociate in significant amounts, leading to large hydrogen contents which are set free. This hydrogen mainly effuses out of the SiN_x:H layers into the atmosphere, however, a small fraction also diffuses into the silicon bulk. At the maximum applied peak temperature of 830 °C, the hydrogen loss is maximal, despite a reduction of hydrogen introduced into the silicon bulk (see Figure 2a). This hydrogen loss can probably be assigned to the reduction of the atomic density of the SiN_x:H layer during RTA, because the nitrogen atoms make a greater contribution to the atomic density.[26] Our FTIR measurements show that after the RTA step at 830 °C, the Si—N bond concentration decreases by 39.4% and so does the atomic density. As a consequence, the equilibrium shifts to the side of the effusion of the hydrogen into the atmosphere (hydrogen loss) and less hydrogen diffuses into the silicon bulk. This is also consistent with an increased blistering at firing temperatures exceeding 800 °C, as can be seen in Figure 2c. Figure 2c shows the blistered area fraction (BAF) of the different SiN_x:H layers as a function of the peak temperature. The BAF values were determined from light microscopy images (see Figure S1, Supporting Information), where we manually determined the fraction of blistered areas on each sample. The decrease in the measured bulk hydrogen content as a function of peak temperature for ϑ_{peak} values beyond the maximum hydrogen content (see Figure 2a) can be obviously correlated with an increased blistering (see Figure 2c) of the SiN_x:H layers. Consequently, blistering seems to be a hydrogen loss mechanism occurring in our samples at the highest peak temperatures.

To examine the hydrogen barrier properties of Al_2O_3 films[18] in-between the hydrogen-rich SiN_x:H layer and the crystalline silicon bulk, in the following we apply the SiN_x layer with $n = 2.3$, which led to the largest hydrogen content in the silicon wafer after RTA (in Figure 2a). The Al_2O_3 layer thickness is varied in the range between 5 and 25 nm (group B, see Experimental Section). To determine the total hydrogen concentration in the silicon bulk, the fired float-zone silicon (Fz-Si) samples are dark-annealed at 160 °C and their resistivity change is measured until saturation, from which the total hydrogen content in the silicon bulk is calculated.

Figure 3 shows the evolution of the bulk resistivity ρ versus the annealing time for exemplary samples of group B, fired at 770 °C. The sample with 5 nm thick Al_2O_3 saturates at the highest resistivity, demonstrating that the highest hydrogen content is diffused into the silicon bulk. Increasing the thickness of the Al_2O_3 layer reduces the resistivity increase due to a lower hydrogen content diffusing into the silicon bulk. Above a layer thickness of 20 nm, the resistivity increase lies within the measurement uncertainty and therefore only negligible hydrogen diffuses into the silicon bulk, clearly proving that ALD-Al_2O_3 acts as a highly effective hydrogen diffusion barrier.

Figure 4 shows the total hydrogen concentrations $[H_{tot}]$ as a function of the Al_2O_3 thickness for three different applied peak temperatures during RTA. Without an Al_2O_3 interlayer (samples of group A), we measure total hydrogen concentrations of 0.5×10^{15} cm^{-3} for an RTA peak temperature of 680 °C, 1.4×10^{15} cm^{-3} for $\vartheta_{peak} = 770$ °C, and 2×10^{15} cm^{-3} for $\vartheta_{peak} = 800$ °C. Inserting only a 5 nm thin ALD-Al_2O_3 interlayer already drastically reduces $[H_{tot}]$ by a factor of five at

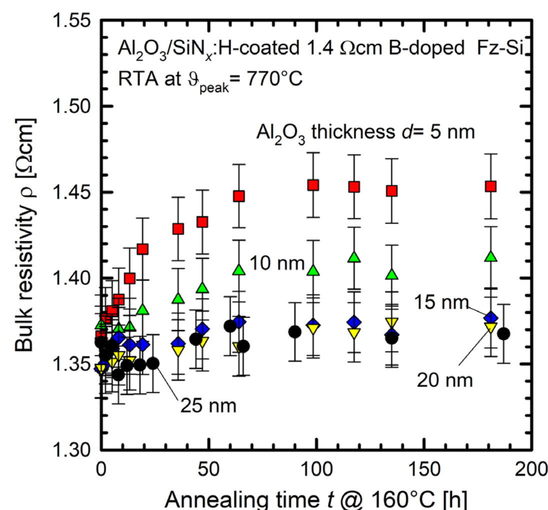

Figure 3. Evolution of the bulk resistivity ρ of Al_2O_3/SiN_x:H-coated 1.4 Ω cm boron-doped float-zone silicon (Fz-Si) samples with different Al_2O_3 thicknesses d between 5 and 25 nm as a function of the annealing time at 160 °C in the dark after rapid thermal annealing (RTA). The composition of the SiN_x layers (refractive index $n = 2.3$) and the rapid thermal annealing (RTA) peak temperature ($\vartheta_{peak} = 770$ °C) are the same for all samples. The sample with 5 nm thick Al_2O_3 layer shows the highest resistivity increase and hence the highest hydrogen content in the silicon bulk. With increasing Al_2O_3 thickness, the hydrogen content in the silicon bulk shows a pronounced decrease.

© 2020 The Authors. Published by Wiley-VCH GmbH

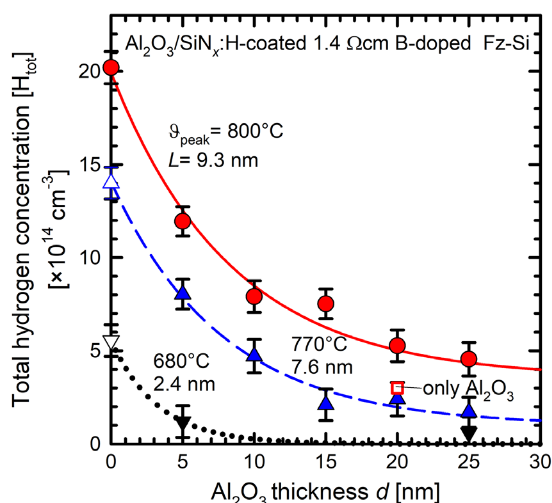

Figure 4. Total hydrogen concentration [H_{tot}] of Al_2O_3/SiN_x ($n = 2.3$) coated 1.4 Ω cm boron-doped float-zone silicon (Fz-Si) samples after rapid thermal annealing (RTA) treatment as a function of Al_2O_3 thickness for three different peak temperatures ϑ_{peak} (uncertainty of measured peak temperatures is ±10 °C). The solid lines are exponential decay fits to extract the diffusion length L of hydrogen in Al_2O_3. The open triangles are taken from Figure 2 and the open square is measured on a wafer coated only by 20 nm of Al_2O_3 and omitting the SiN_x:H.

$\vartheta_{peak} = 680$ °C. Thicker Al_2O_3 layers practically completely prevent hydrogen from diffusing through the Al_2O_3 layer at $\vartheta_{peak} = 680$ °C. The higher applied peak temperatures of $\vartheta_{peak} = 770$ °C and 800 °C require thicker Al_2O_3 layers to lead to the same degree of preventing hydrogen from diffusing into the silicon bulk. To reduce [H_{tot}] by a factor of ≈5 at a peak temperature of 770 °C, an ≈15 nm thick Al_2O_3 layer is required, and at $\vartheta_{peak} = 800$ °C, an ≈20 nm thick Al_2O_3 layer is necessary. Without any SiN_x:H layer on top of the Al_2O_3 (which itself contains about 1–2 at% hydrogen[3]), a very low hydrogen content diffuses from the Al_2O_3 layer into the silicon bulk, as shown in Figure 4 for a sample with 20 nm Al_2O_3 fired at a peak temperature of 800 °C (red open square).

Fitting exponential decay curves (lines in Figure 4) to the measured data, the diffusion length L of hydrogen in Al_2O_3 is determined for each applied temperature ϑ_{peak}. At the higher RTA peak temperatures of about 800 and 770 °C, the in-diffused hydrogen content as a function of Al_2O_3 thickness saturates at a non-zero hydrogen concentration, because the Al_2O_3 layer provides some hydrogen itself. We measured an in-diffused hydrogen content for a sample coated only with 20 nm of Al_2O_3 (data point "only Al_2O_3") treated at a RTA peak temperature of ≈800 °C. The 680 °C RTA peak temperature is too low for the hydrogen in-diffusion from the Al_2O_3 into the silicon bulk, leading to a hydrogen content below the detection limit of our method. Therefore, the exponential decay fit for the black data points saturates for Al_2O_3 thicknesses >10 nm at zero. At the highest applied ϑ_{peak} of 800 °C, the diffusion length of hydrogen in Al_2O_3 amounts to (9.3 ± 0.3) nm. The hydrogen diffusion length is reduced to $L = (7.6 \pm 0.4)$ nm by reducing ϑ_{peak} by only 30 °C and the lowest ϑ_{peak} of 680 °C leads to a diffusion length of only (2.4 ± 0.1) nm, demonstrating that already ultrathin Al_2O_3 layers of only a few nm can be applied as a highly effective hydrogen diffusion barrier. This knowledge can be applied to the production of silicon solar cells, where it has recently been shown that introduction of hydrogen into the silicon bulk during the contact firing step can lead to a severe light and elevated temperature-induced degradation (LeTID) in efficiency.[16,27] The results presented in this letter can therefore be applied to avoid hydrogen in-diffusion by implementing Al_2O_3 layers optimized as hydrogen barriers. Note that this would also be consistent with recent reports by other groups.[16,28]

In conclusion, the total hydrogen concentration diffused into crystalline silicon from hydrogen-rich SiN_x:H layers during RTA has been measured as a function of RTA peak temperature, SiN_x:H composition, and Al_2O_3 thickness in an Al_2O_3/SiN_x:H stack. The total hydrogen concentration [H_{tot}] diffused into the silicon bulk was found to show a maximum as a function of the RTA peak temperature ϑ_{peak}. The ϑ_{peak} position of the maximum depends on the composition of the SiN_x layer, as characterized by the refractive index n measured by ellipsometry at a wavelength of 633 nm. The largest total hydrogen concentration [H_{tot}] of 2×10^{15} cm^{-3} was detected for a silicon-rich SiN_x layer with a refractive index of $n = 2.3$ at $\vartheta_{peak} = 800$ °C. Increasing the peak temperature above 800 °C led to a decrease in [H_{tot}] due to a decrease in the atomic density of the SiN_x layer, as shown by FTIR measurements. A drastic reduction of [H_{tot}] was achieved by introducing an ALD-Al_2O_3 layer in-between the silicon-rich SiN_x:H layer and the crystalline silicon surface. A 5 nm thick Al_2O_3 layer led to a reduction of [H_{tot}] by a factor of ≈5 at $\vartheta_{peak} = 680$ °C and even thicker Al_2O_3 layers practically completely prevented hydrogen from diffusing through the Al_2O_3 layer. Thicker Al_2O_3 layers were found to be necessary at higher RTA peak temperatures for preventing hydrogen from diffusing into the silicon bulk. For example, to reduce [H_{tot}] by a factor of 4 at $\vartheta_{peak} = 800$ °C, a 20 nm thick Al_2O_3 layer was required. Our results clearly demonstrate that ultrathin Al_2O_3 layers of only a few nm are highly effective hydrogen diffusion barriers. The adaption of such diffusion barriers could be useful in the production of silicon solar cells, where hydrogen in-diffusion into the silicon bulk has recently been identified as one major reason for detrimental light-induced degradation effects.[16,27,28]

Experimental Section

Sample Preparation: We used (100)-oriented 300 μm thick 1.4 Ω cm boron-doped Fz-Si wafers. The 6″ Fz-Si wafers were first cleaned with a surface-active agent. Subsequently, they were etched back to a thinner sample thickness in a potassium hydroxide solution followed by an RCA cleaning sequence. To remove possible remaining metallic contaminants in the silicon bulk, the wafers were then phosphorus gettered in a quartz tube furnace using $POCl_3$ at 850 °C. The resulting phosphosilicate glass and n^+-regions (n^+ sheet resistance ≈80 Ω sq^{-1}) on both wafer surfaces were removed by hydrofluoric acid and potassium hydroxide solutions, respectively, so that the final wafer thickness amounts to (142 ± 3) μm. After cutting the Fz-Si wafers into 2.49 × 2.49 cm^2 large samples and another RCA cleaning, the samples were split into two groups. In group A, the surfaces were symmetrically passivated with single layers of SiN_x:H coated by means of remote plasma-enhanced chemical vapor deposition (remote PECVD) at 400 °C on both sample surfaces in a Plasmalab 80 Plus System (Oxford Instruments). The ammonia gas flow was set constant at

 © 2020 The Authors. Published by Wiley-VCH GmbH

200 sccm and the nitrogen gas flow was set at 100 sccm. To vary the composition of the SiN_x:H layers, and hence their refractive index n (measured by ellipsometry at a wavelength of $\lambda = 633$ nm), we applied different silane gas flows of 1.2 sccm (resulting in $n = 1.9$), 8.5 sccm ($n = 2.3$), and 15 sccm ($n = 2.7$). All SiN_x:H films had the same thickness of (130 ± 4.5) nm by adjusting the deposition time. The samples of group B were symmetrically coated with Al_2O_3/SiN_x:H stacks on both surfaces. The Al_2O_3 layers were deposited by means of plasma-assisted atomic layer deposition (PA-ALD) in a FlexAL system (Oxford Instruments) at 200 °C using trimethylaluminum (TMA) and an oxygen plasma for oxidation in each cycle. By varying the number of cycles, the Al_2O_3 thickness was adjusted between 5 and 25 nm to systematically examine the impact of the Al_2O_3 thickness on the hydrogen diffusion into the silicon bulk during the RTA step. For all samples of group B, we applied silicon-rich SiN_x:H layers ($n = 2.3$), because these layers showed the maximum in-diffused hydrogen concentration in the samples of group A. In the final process step, all samples received an RTA step in an industrial infrared conveyor-belt furnace (DO-FF-8.600-300, centrotherm AG) at different set-peak temperatures at a belt speed of 6.8 m min^{-1}. The actual sample temperature was measured by a type-K thermocouple (KMQXL-IMo50G-300, Omega) in combination with a temperature tracker (DQ1860A) from Datapaq. The measured peak temperature ϑ_{peak} was varied for the samples from group A between 606 and 860 °C and in group B between 680 and 800 °C.

Experimental Details: We measured the hydrogen concentration introduced into the silicon bulk by a very sensitive method, which was based on the formation of BH pairs upon prolonged annealing the samples, thereby increasing the specific resistivity ρ of the boron-doped silicon until saturation.[21]

Supporting Information

Supporting Information is available from the Wiley Online Library or from the author.

Acknowledgements

The authors thank C. Marquardt for sample processing. This work was funded by the German State of Lower Saxony and the German Federal Ministry of Economics and Energy within the research project LIMES (Contract no. 0324204D). The content is the responsibility of the authors. Open access funding enabled and organized by Projekt DEAL.

Conflict of Interest

The authors declare no conflict of interest.

Keywords

aluminum oxide, defects, diffusion, hydrogen, silicon

Received: July 27, 2020
Revised: September 18, 2020
Published online: October 2, 2020

[1] R. Lo Nigro, E. Schilirò, G. Greco, P. Fiorenza, F. Roccaforte, *Thin Solid Films* **2016**, *601*, 68.
[2] J. Schmidt, R. Peibst, R. Brendel, *Sol. Energy Mater. Sol. Cells* **2018**, *187*, 39.
[3] B. Hoex, J. Schmidt, P. Pohl, M. C. M. van de Sanden, W. M. M. Kessels, *J. Appl. Phys.* **2008**, *104*, 44903.
[4] Y. Yue, Y. Hao, J. Zhang, J. Ni, W. Mao, Q. Feng, L. Liu, *IEEE Electron Device Lett.* **2008**, *29*, 838.
[5] R. Suri, C. J. Kirkpatrick, D. J. Lichtenwalner, V. Misra, *Appl. Phys. Lett.* **2010**, *96*, 42903.
[6] T. Dullweber, J. Schmidt, *IEEE J. Photovoltaics* **2016**, *6*, 1366.
[7] D. Bredemeier, D. C. Walter, R. Heller, J. Schmidt, in *Proc. 36th EUPVSEC*, Marseille, France **2019**, p. 112.
[8] J. Hong, W. M. M. Kessels, W. J. Soppe, A. W. Weeber, W. M. Arnoldbik, M. C. M. van de Sanden, *J. Vac. Sci. Technol. B* **2003**, *21*, 2123.
[9] B. J. Hallam, S. R. Wenham, P. G. Hamer, M. D. Abbott, A. Sugianto, C. E. Chan, A. M. Wenham, M. G. Eadie, G. Xu, *Energy Procedia* **2013**, *38*, 561.
[10] S. J. Pearton, J. W. Corbett, T. S. Shi, *Appl. Phys. A* **1987**, *43*, 153.
[11] B. L. Sopori, X. Deng, J. P. Benner, A. Rohatgi, P. Sana, S. K. Estreicher, Y. K. Park, M. A. Roberson, *Sol. Energy Mater. Sol. Cells* **1996**, *41/42*, 159.
[12] D. Bredemeier, D. C. Walter, J. Schmidt, *Sol. RRL* **2018**, *2*, 1700159.
[13] P. M. Weiser, E. Monakhov, H. Haug, M. S. Wiig, R. Søndenå, *J. Appl. Phys.* **2020**, *127*, 65703.
[14] D. Chen, P. Hamer, M. Kim, C. Chan, A. Ciesla nee Wenham, F. Rougieux, Y. Zhang, M. Abbott, B. Hallam, *Sol. Energy Mater. Sol. Cells* **2020**, *207*, 110353.
[15] R. Eberle, W. Kwapil, F. Schindler, S. W. Glunz, M. C. Schubert, *Energy Procedia* **2017**, *124*, 712.
[16] T. Niewelt, M. Selinger, N. E. Grant, W. Kwapil, J. D. Murphy, M. C. Schubert, *J. Appl. Phys.* **2017**, *121*, 185702.
[17] S. Wilking, A. Herguth, G. Hahn, *J. Appl. Phys.* **2013**, *113*, 194503.
[18] A. A. Dameron, S. D. Davidson, B. B. Burton, P. F. Carcia, R. S. McLean, S. M. George, *J. Phys. Chem. C* **2008**, *112*, 4573.
[19] V. V. Voronkov, R. Falster, *Phys. Status Solidi B* **2017**, *254*, 1600779.
[20] R. E. Pritchard, J. H. Tucker, R. C. Newman, E. C. Lightowlers, *Semicond. Sci. Technol.* **1999**, *14*, 77.
[21] D. C. Walter, D. Bredemeier, R. Falster, V. V. Voronkov, J. Schmidt, *Sol. Energy Mater. Sol. Cells* **2019**, *200*, 109970.
[22] D. Bredemeier, D. C. Walter, R. Heller, J. Schmidt, *Phys. Status Solidi RRL* **2019**, *13*, 1900201.
[23] Z. Yin, F. W. Smith, *Phys. Rev. B* **1990**, *42*, 3666.
[24] C. Boehme, G. Lucovsky, *J. Vac. Sci. Technol. A* **2001**, *19*, 2622.
[25] S. Wilking, S. Ebert, A. Herguth, G. Hahn, *J. Appl. Phys.* **2013**, *114*, 194512.
[26] A. F. Holleman, E. und Nils Wiberg, G. Fischer, *Lehrbuch der Anorganischen Chemie*, Walter de Gruyter, Berlin **2007**.
[27] J. Schmidt, D. Bredemeier, D. C. Walter, *IEEE J. Photovoltaics* **2019**, *9*, 1497.
[28] U. Varshney, B. Hallam, P. Hamer, A. Ciesla, D. Chen, S. Liu, C. Sen, A. Samadi, M. Abbott, C. Chan, B. Hoex, *IEEE J. Photovoltaics* **2020**, *10*, 19.

© 2020 The Authors. Published by Wiley-VCH GmbH